

# Measurements of Radiation Power from High Z Impurities with TESPEL and Comparison with Theoretical Calculations

Shigeru SUDO<sup>1,2)</sup>, Naoki TAMURA<sup>1)</sup>, Chihiro SUZUKI<sup>1)</sup>,  
Hisamichi FUNABA<sup>1,2)</sup> and Izumi MURAKAMI<sup>1,2)</sup>

<sup>1)</sup>National Institute for Fusion Science, 322-6 Oroshi-cho, Toki 509-5292, Japan

<sup>2)</sup>The Graduate University for Advanced Studies, Hayama, Kanagawa 240-0193, Japan

(Received 30 September 2014 / Accepted 11 November 2014)

Utilizing the advantage of the Tracer-encapsulated Solid Pellet (TESPEL) injection method, the radiation power emitted from heavy atoms such as tungsten is measured knowing the total amount of the heavy atoms. The experimentally obtained radiation power is compared with the theoretical calculations. The TESPEL method is found to be useful for evaluating the absolute radiation power from the heavy atoms, although the present status is preliminary and further data should be accumulated.

© 2014 The Japan Society of Plasma Science and Nuclear Fusion Research

Keywords: TESPEL, pellet, tracer, impurity, radiation power

DOI: 10.1585/pfr.9.1202147

In magnetic confined plasmas, the accumulation of impurities is one of the subjects of concern. It can cause cooling down of the fusion plasma and also dilution of the fusion fuel. On the other hand, the localization of an adequate impurity amount in the plasma edge might cause appropriate radiation power which could mitigate the heat load on the divertor plate. From this viewpoint, a Tracer-encapsulated Solid Pellet (TESPEL) injection method has been developed [1].

In this paper, we report on the measurement results of the radiation power from the heavy atoms. For this, we used the following advantages of TESPEL: (a) direct local deposition of tracers inside the plasma is possible; (b) the deposited amount of the tracer inside the plasma can be known precisely; and (c) a relatively wide selection of tracer materials is possible.

The total radiation power  $P$  due to some amount of impurity in a plasma is written as:

$$P = \int L(T_e(r))n_e(r)n_z(r)dV, \quad (1)$$

where  $L$  is the radiative power loss rate, and  $n_e$  and  $n_z$  are the electron density and the impurity density, respectively. Generally  $L$  depends on the electron temperature and density, but the density dependence is small for high Z impurities with the plasma parameters concerned here. For the calculation of the radiative cooling rate  $L$ , Post *et al.* uses an average ion model (AIM) which is explained well in Appendix A of Ref. [2]. In the model, an average ion was obtained by averaging statistically all possible charge states of an element, and the radiation rate and the mean charge state in coronal equilibrium were calculated. The AIM model is available for our interested

author's e-mail: sudo@ms.nifs.ac.jp

plasma parameter range ( $1 \times 10^{18} \text{ m}^{-3} \leq n_e \leq 1 \times 10^{21} \text{ m}^{-3}$ ,  $100 \text{ eV} \leq T_e \leq 100 \text{ keV}$ ). The more precise treatment for  $W$  with the Cowan code using a configuration averaged model (CAM) was performed by Pütterich *et al.* [3]. They performed the level-resolved calculations, and thus could give the spectral contributions to the radiative cooling rates. Their calculations were done only for  $W$ . As the radiative cooling rates for  $W$  given by Post agree relatively well with those given by Pütterich considering the accuracy, we will compare the experimental data with the calculated data given by Post.

Utilizing the advantage of the localized deposition of the tracer, the deposition location is assumed here as  $r_*$  in the early phase for simplicity,

$$n_z(r) = n_z \delta(r - r_*), \quad (2)$$

and

$$\int n_z(r)dV = N_z. \quad (3)$$

The total amount of the tracer deposited by a TESPEL is precisely determined as  $N_z$  (which is due to the advantage of TESPEL), then,

$$P \sim L(T_e(r_*))n_e(r_*)N_z. \quad (4)$$

For  $P$ , we use the bolometric power obtained experimentally. Thus, we can obtain  $L$  experimentally by knowing  $P$ ,  $n_e(r_*)$ , and  $N_z$ .

The local electron temperature and density are approximated in this paper as those at the tracer deposition location, although more accurate comparison may be possible using somewhat broadened profiles according to the diffusion of the tracers. The temporal development of the bolometric power  $P_{\text{bol}}$  for the average bulk electron density

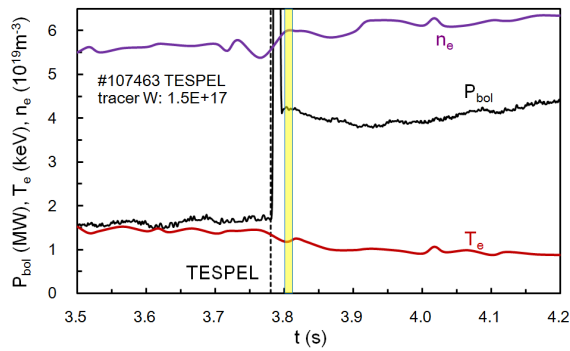


Fig. 1 Temporal developments of  $P_{\text{bol}}$  and the local value of  $T_e$  and  $n_e$  at  $r_{\text{eff}} = 0.40$  m. The TESPEL having the tungsten tracer is injected at the timing denoted by the dotted line.

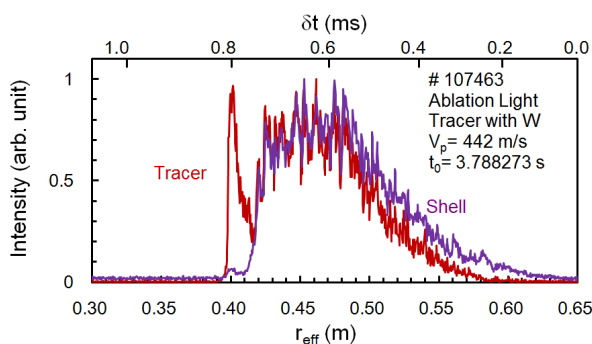


Fig. 2 Temporal developments and corresponding locations of the ablation light emissions through the filters for the shell and the tracer, respectively.  $\delta t$  stands for the time passed after the time  $t_0$ .

of  $n_e = 5.4 \times 10^{19} \text{ m}^{-3}$  with a tungsten tracer is shown in Fig. 1. The amount of the tungsten tracer is  $1.5 \times 10^{17}$  particles. The local electron temperature and density measured by a Thomson scattering system at  $r_{\text{eff}} = 0.40$  m (the deposition location of the W tracer as seen in Fig. 2) are also shown, where  $r_{\text{eff}}$  is the radius of the equivalent circle cross section based on the equilibrium code calculation. The temporal developments of the ablation light through the filters for the shell ( $H\alpha$ ) and the tracer are shown in Fig. 2 by normalizing with the peak value. As the spectral width of the filter for W I (400.9 nm) is broad (FWHM of 2.0 nm), the background light penetrates through the filter, but the local deposition (2~3 cm) of the tracers has already been confirmed in the previous experiments with a high resolution spectrometer with a sufficient time resolution [4]. The bolometric power increase due to the TESPEL outer layer of polystyrene is negligible. The increase of the bolometric power and the local electron temperature and density are taken at the timing indicated by a hatched bar in Fig. 1 (in the 20-30 ms after the TESPEL injection). Thus, the experimentally obtained  $L$  value can be compared with the calculated data.

The dependence of  $L$  on the electron temperature

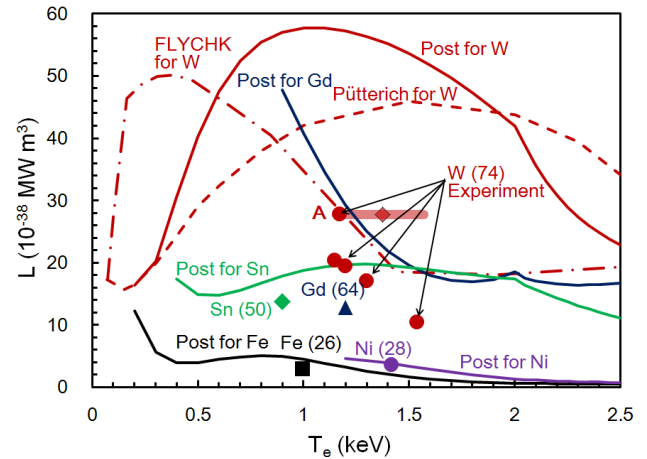


Fig. 3 Radiation power loss rates given in Refs. [2, 3, 5]. The experimental data of W, Gd, Sn, Ni, and Fe are shown by symbols. The bar next to “A” indicates the broadening of the electron temperature experienced by W particles due to the assumed particle diffusion in  $\sim 30$  ms.

given by Post is plotted with solid lines in Fig. 3. The experimental data are shown by symbols for Fe, Ni, Sn, Gd, and W. “A” denotes the data obtained in the case of Fig. 1. The data for W given by Pütterich and also by the FLYCHK code [5] are shown for reference. The ratios of the experimental data to the data given by Post are 0.6 for Fe, 0.9 for Ni, 0.8 for Sn, 0.5 for Gd, and 0.2-0.5 (0.3 in average) for W. The discrepancy seems relatively small, considering the accuracy of the experiments ( $\sim 50\%$ ) and the model calculations (factor of 2~4).

The experimentally obtained data of W in the range of  $T_e = \sim 1$  keV indicates that the radiation power from W with the particle amount of  $1.6 \times 10^{19}$  (5 mg) in the plasma periphery of  $n_e = \sim 1 \times 10^{20} \text{ m}^{-3}$  can reach  $\sim 400$  MW in a fusion reactor. Such a quantity is within a practical value for the radiation cooling in the plasma periphery. When it is necessary to put the impurities locally in some narrow layer in the plasma edge region, it may be useful to use a TESPEL/TECPEL configuration [6], namely the outer layer of polystyrene or cryogenic solid hydrogen and the inner core of W. If Kr or Xe is an option for the radiator, a cryogenic solid Kr or Xe with a larger amount than the case of W can be used by covering with solid hydrogen.

## Acknowledgments

The authors would like to thank the LHD Experiment Group for their support in the experiment. This work is supported by a Grant-in-Aid for Scientific Research (B) No.23360415 from JSPS Japan and budgetary Grant-in-Aid ULHH012 provided by NIFS.

- [1] S. Sudo *et al.*, Plasma Fusion Res. **9**, 1402039 (2014).
- [2] D.E. Post *et al.*, Atom. Data and Nucl. Data Tables **20**, 397 (1977).

[3] T. Pütterich *et al.*, Nucl. Fusion **50**, 025012 (2010).  
[4] S. Sudo *et al.*, Plasma Phys. Control. Fusion **45**, A425 (2003).

[5] <http://www-amdis.iaea.org/FLYCHK/>  
[6] S. Sudo *et al.*, Rev. Sci. Instrum. **76**, 053507 (2005).